

# A Novel Fuzzy Logic Based GPSO PR Controller for Minimization of Steady State Errors and Harmonics in Standalone Wind and Solar PV Hybrid System

G. N. S. Vaibhav\*<sup>‡</sup>, B. S. Srikanthan\*\*

\* Electrical & Electronics Engineering, Research Scholar, NIE Institute of Technology, Mysuru, 570018

\*\* Electrical & Electronics Engineering, Associate Professor, NIE Institute of Technology, Mysuru, 570018

(vaibhavnaidu.naidu@gmail.com, bssrikanthan@gmail.com)

<sup>‡</sup> G N S Vaibhav; Dr B S Srikanthan, 570018, Tel: +91 7989209265,

vaibhavnaidu.naidu@gmail.com

*Received: 10.09.2022 Accepted: 05.11.2022*

**Abstract-** Standalone or off-grid electricity system requires continuous, sustainable and reliable power supply. To address this challenge, a hybrid renewable energy system which includes combination of wind and solar energy sources to achieve better system efficiency as well as improved balance in energy supply. To provide a constant output irrespective of energy fluctuations a Battery Energy Storage System (BESS) needs to be incorporated in the stand-alone system. However, power conversion and power management in standalone hybrid renewable energy system are not free from harmonics and steady state errors. Hence an energy management system with an appropriate controller has to be developed to reduce the harmonics, steady state errors and as well as to provide a constant output voltage. A novel fuzzy logic based GPSO (genetic particle swarm optimization) PR (proportional resonant) controller for hybrid wind and solar PV generation system is proposed in this paper and a comparative analysis is effectively done to calculate the performance of Fuzzy GPSO based PR controller with fuzzy logic-based PI, PR controllers where steady state errors and harmonics under different load circumstances are considered. The proposed standalone hybrid renewable energy system design and modelling is experimented in MATLAB/SIMULINK to validate the authenticity of results.

**Keywords** Solar Power, Wind Power, Hybrid Renewable Energy System, Standalone Loads, PI controller, PR controller, Fuzzy Logic, Particle Swarm Optimization, Steady State Errors, Harmonics, Simulation.

## 1. Introduction

A hybrid renewable energy method is a power method where multiple renewable energy resources are combined together which produces electricity that is highly consistent and also economical. The energy habituation devices act like a controller together with the option of a power saving system. They can operate in grid-connected or isolated mode, with the possibility of storage and backup from more traditional sources such as diesel generators. HRES may be a feasible exploitation choice in distant areas where traditional energy production methods are not offered or not commercial, to

attain the customers requirement for a trustworthy delivery of energy. Furthermore, HRES is a less expensive, dependable, and ecologically favourable sustainable energy source capable of significantly lowering total lifecycle costs. As a result, optimization-based control approaches are implemented in HRES.

To accomplish electromagnetic power transfer with control, a variety of electrical devices can be used, with its own set of benefits and drawbacks. The research in the area of permanent-magnet synchronous generators (PMSGs) has gained popularity as the tiny trade winds function in remote as

well as in isolated places. PMSG functions effectively in less-energy wind power scenarios as it is light weight and it has better power concentration. It has the additional advantage as it does not require any external excitation current. A diode bridge rectifier is incorporated at the generator terminals as it does not require any externally applied electric current which finally results good amount cost savings. The system design explored in this work is based on a PMSG connected to the dc link via a diode bridge rectifier.

The energy sources in this paper are wind and solar. The wind turbine is connected to the PMSG that converts involuntary power into electrical power. The generated ac power is converted to dc using an ac-dc converter and also the voltage ratio is increased by a dc-dc boost converter. Solar PV array generate the power at the maximum power level during variable solar irradiance. Two power resources are linked by a common dc-bus line. As a result, the system is transformed into a hybrid standalone solar-wind energy system. When the wind speed goes high, the electricity which is generated by the wind turbine remains higher, and during the sunny days, when the temperature is high, the power generated by the solar panels will turn to be higher.

As a result, the load balancing issue is caused by the active power provided through the wind turbine as well as solar panel. To moderate output fluctuations, Energy Storage Systems (ESS) are used. This work employs the Battery Energy Storage System (BESS) to save surplus power and also to deliver when it is needed.

In most standalone HRES, coordinated controller techniques are employed for power management. Usually, PI controller is preferred for effective power management. However, PI controllers have some drawbacks. The output of the PI controller is poor under unbalanced load scenarios. The gain supplied through the PI controller is inadequate at higher frequencies. When dynamic load changes occur, these traditional coordinated controllers plagued transient issues. The Proportional Resonant (PR) controller eliminates these flaws.

However, when dynamic load changes occur, the PR controller was subjected to transitory circumstances. Fuzzy logic based Proportional Resonant controller (Fuzzy PR) is being developed to solve this problem. Fuzzy PR is a basic rule-based concept which is used for self-consumption optimization where the storage device is charged when generated power is in surplus state and is discharged when the load power becomes high. Wind energy follows the same procedure. If there is no feed-in limit, the power supplied to the load will fluctuate between zero and nominal power. It potentially increases the steady state error. If there is a feed-in limit, PV and wind power are restricted and it reduces PV, wind power supply to load and increases the harmonics of the load voltage and current. Steady state error and harmonics are the two major issues in standalone HRES.

In general, for high nonlinear applications like HRES finding parameters such as scaling gains and membership function in fuzzy is difficult. So only fuzzy logic-based PR controller is not sufficient to minimize the steady state error and harmonics. The Fuzzy PR approach is paired with the Genetic Particle Swarm Optimization (GPSO) approach to tackle this issue. The steady state error and harmonics are decreased by combining a Fuzzy PR controller with a GPSO.

The effectiveness and superiority of the hybrid fuzzy GPSO PR controller over the conventional controllers are demonstrated in this paper by comparing it with fuzzy logic-based PI, PR controllers.

## 2. Proposed System

The solar energy and the wind energy is converted to electrical energy by using the PV array and a wind turbine generator (WTG) set. The variable AC voltage from the PMSG is converted to DC by using a diode bridge rectifier unit which is then given to Dc-Dc boost converter. Solar PV output voltage is then linked to Dc-Dc boost converter with the help of the common DC bus line. A battery is linked to Dc-Dc converter and also to the load. The surplus energy created is stored for future use. The DC-DC voltage of boost converter is thereby increased with the required quality and it is further converted to AC using inverter with less steady state errors and harmonics by a Fuzzy logic based GPSO PR controller. The entire configuration flow of the proposed model is mentioned in the below Fig. 1.

### 2.1. Wind Turbine Model

A wind turbine is defined by the power-speed characteristics. The amount of power extracted from a wind turbine is calculated by the quantity of wind available, the machine’s power curve, and its ability to react to wind fluctuations. Because wind turbines are mostly dependent on wind velocity and rotor blade radius, they are placed on massive looms to maximum energy production.

Fig. 2 depicts a schematic layout of a WECS with a BEES installed at the dc bus. The battery is connected to the system via a unidirectional proposed converter. The mechanical power extracted by the turbine can be expressed using Eq.1. It’s used to create wind turbine models that are based on the link among wind speed as well as power.

$$P_{wind} = 0.5\rho AV^3 C_p(\lambda, \beta) \tag{1}$$

$\rho$  is the air density, The rotor surface is A, and the wind speed is V. The tip speed margin ( $\lambda$ ) as well as angular position ( $\beta$ ) determines  $C_p$ , which stands for coefficients of energy. Equation 2 describes the aerodynamic torque acting on the rotor blades.

$$T = 0.5 \rho C_t \tag{2}$$

$$C_t = C_p / \lambda \tag{3}$$

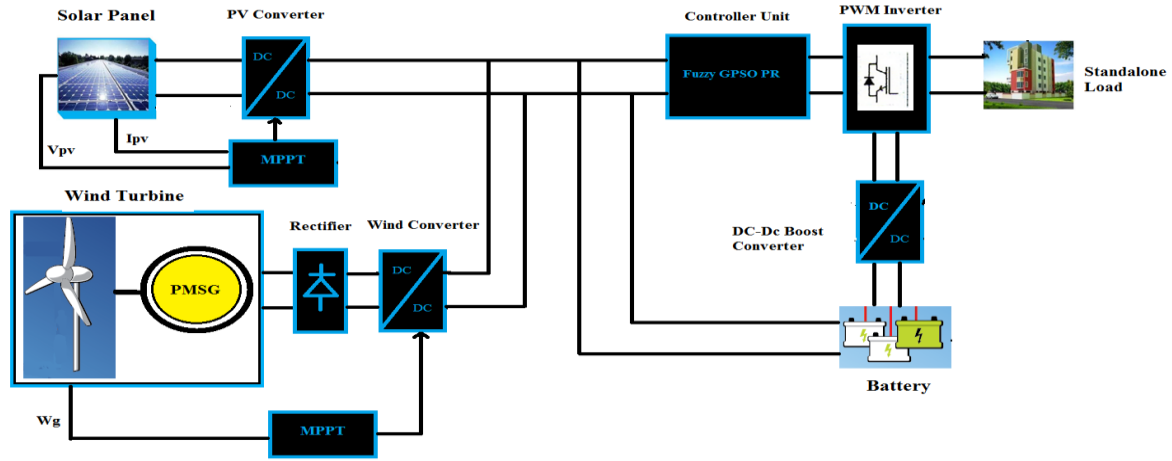


Fig. 1. Block Diagram of the Proposed System

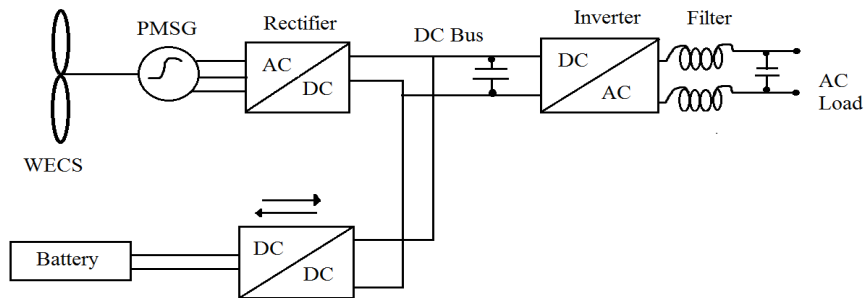


Fig. 2. Schematic Layout of the Wind Turbine Model in Proposed System

where  $C_t$  is the torque coefficient. The equation of  $C_p$  in terms of  $\lambda$  is given as

$$C_p = 0.00055 - 0.012 + 0.097 - 0.2 \lambda + 0.11 \quad (4)$$

2.2. Permanent Magnet Synchronous Generator (PMSG) Model

The mechanical torque applied to a permanent magnet machine determines its mode of operation. The machine will work as a generator if the torque is unconstructive and as a motor if the torque is optimistic. The benefit of employing a PMS is that it does not require a capacitor bank for excitation. The stator voltage equations for PM machines in direct and quadrature axes are written as Eq. 5 and 6.

$$v_d = i_d R_s + L_d \omega L q i_q \quad (5)$$

$$v_q = i_q R_s + L_q \omega L d i_d + \omega \Psi_f \quad (6)$$

where  $v_d$  is the voltage on the direct axes of the stator,  $v_q$  - voltage in the quadrature axes of the stator,  $R_s$  stands for stator confrontation,  $i_d$  - current in straight axis stator,  $i_q$  - stator current quadrature axis,  $\omega$  - frequency of angular motion  $\Psi_f$  stands for instability connection, The torque produced through PMSG is

$$T_g \text{ or } T_e = - P (\Psi_f i_q + L_d - L_q) i_q \quad (7)$$

where  $P$  - pole couples. The equation of movement is known as

$$\frac{dw}{dt} = \frac{1}{J} (T_e - T_m) \quad (8)$$

$$\frac{d\theta}{dt} = \omega \quad (9)$$

$J$  stands for rotational inertia of the generator,  $\theta$  is rotor position,  $T_m$  is the mechanical torque and  $T_g$  or  $T_e$  is the electromagnetic torque. A diode rectifier is used to convert the generator output to DC, as displayed in Fig. 1. The DC filter is composed of a series reactor and a shunt capacitor, Eq.10 gives the capacitor voltage across the dc bus. The DC power that passes from side to side the filter is equal to

$$\frac{dVdC}{dt} = \frac{I_r - I_{in}}{C} \quad (10)$$

$$\frac{dI_r}{dt} = \frac{V_r - V_{in}}{L} \quad (11)$$

where  $V_{in}$  is the inverter's input voltage,  $V_r$  is the rectifier's output voltage,  $I_r$  is the current flowing through the inductor, and  $I_{in}$  is the inverter's side current, and  $C$  and  $L$  are the filter circuit's capacitance and inductance, respectively.

2.3. Maximum Power Transfer Control Technique

In a wind power system, the role of MPPT controller is very important. The MPPT controller calculates the peak power (MPP) on a continuous basis as well as the performance of wind energy under fluctuating wind speeds is modified by the duty cycle of the DC-DC boost converter.

When the wind turbine functions at maximum  $C_p$ , it creates the maximum power. As a result, the rotor speed must be kept at the angle speed proportion's desired value,  $k_{opt}$ . To keep up with the changing wind speed, the rotor speed must change as well.

The peak energy from a wind turbine must be noted as:

$$P_{m_{opt}} = \frac{1}{2} \rho C_p A^* \left( \frac{E W m_{opt}}{\lambda_{opt}} \right)^2 \tag{12}$$

Where,

$$W m_{opt} = \frac{\lambda_{opt} V_w}{R} \tag{13}$$

Therefore, the optimum torque can be given by:

$$T m_{opt} = K_{opt} W m_{opt}^2 \tag{14}$$

Where,

$$K_{opt} = \frac{1}{2} \rho C_p A^* \left( \frac{R}{\lambda_{opt}} \right)^2 \tag{15}$$

For varying wind speeds, Fig. 3 depicts the physical rotational energy as well as the maximum energy produced by a turbine as a relation of rotor speed.

The Fig. 3 shows the wind speed, as there is always a corresponding rotor speed that creates the maximum power  $P_{mopt}$ .

2.4. Solar Power Generation Unit

In a comprehensive hybrid power system, solar power takes precedence in terms of power supply. When solar power is compared to the wind power, the cost of solar power is very low as there is no wear and tear. Though the economic criteria can be ignored, the output power limits from solar power generation system  $P_s$  must be considered.

$$0 \leq P_s(k) \leq P_{s-max}(k) \tag{16}$$

where  $P_{s-max}$  is the maximum output power that a solar power system can produce.

2.5. Proportional-Integral (PI) Controller Design

PI controller is a conventional solution for most of the industrial application because the structure is very simple to understand.

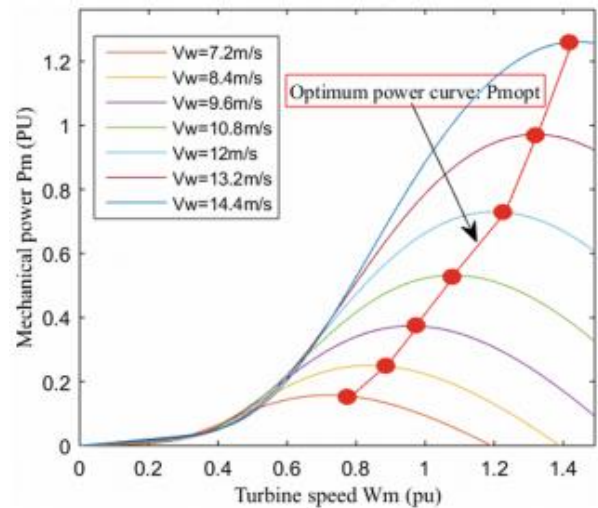


Fig. 3. Turbine power characteristics (Pitch angle beta = 0 deg)

In this study, the PI controller is used in a circuit to control the switching frequency of the switch S. Fig. 4 depicts the proposed control strategy of PI controller. Where:

$$T g_{ref} W m = K_{opt} W m^2 \tag{17}$$

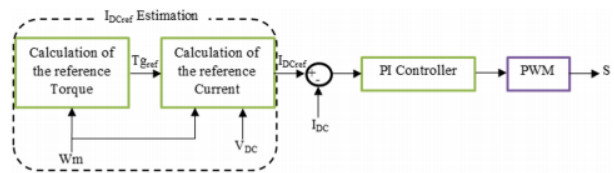


Fig. 4. Block diagram of the PI controller

$$I_{DC_{ref}} = \frac{T g_{ref} W m}{V_{DC}} \tag{18}$$

and

$$F(P) = \frac{I_{DC}(P)}{\alpha(P)} = \frac{V_L}{L_p} \tag{19}$$

The difference between the reference current  $I_{DC_{ref}}$  and the measured current  $I_{DC}$  is utilized to control the output of the Boost converter and the generator torque via a PI controller by varying the duty cycle of the switch S. The gains of the PI controller are calculated using the boost converter's transfer function, which is provided in (19). where  $I_{DC}$  inductor current variation,  $V_L$  output voltage with a disturbed duty cycle,  $L$  inductor value, and  $p$  is the Laplace operator.

2.6. Proportional Resonant Controller

The output signals of power converters are handled by controllers, so designing the controller, including the correct gain, is a challenging issue. In addition, controllers should be capable of rejecting harmonic disturbances and controlling performance at critical frequencies. Because the PI controllers retain a pole (with an unbounded gain) in the zero- frequency state, this controller is incapable of reducing the steady-state error in the fundamental frequency state. Because of this flaw,

PR controllers are utilized instead of PI controllers. The PR controller refers to the combination of proportional and resonant terms. This controller's equation is listed below.

$$C_{PR} = K_p + K_r \frac{s}{s^2 + \omega^2} \tag{20}$$

where,  $\omega$  - frequency response

This type of controller employs a large amount of gain in the resonant frequency region to avoid steady-state mistake when monitoring or refusing the output voltage. For improving harmonic handling performance, a harmonic compensator can be used.

$$C_{HC}(s) = \sum K_h \frac{s}{s^2 + \omega^2} \tag{21}$$

where, h - harmonic order

In that circumstance, better control system presentation is critical, as well as the frequency response must be kept near to the system's frequency. When a system's frequency varies dramatically, adaptive devices can be employed to change the resonant frequency to match the system's frequency.

2.7. Fuzzy GPSOPR Controller

To increase the voltage, the suggested fuzzy logic based GPSOPR controller incorporates the Fuzzy Logic (FL) and GPSO concepts, as well as a PR controller, into one structure as show in Fig. 5.

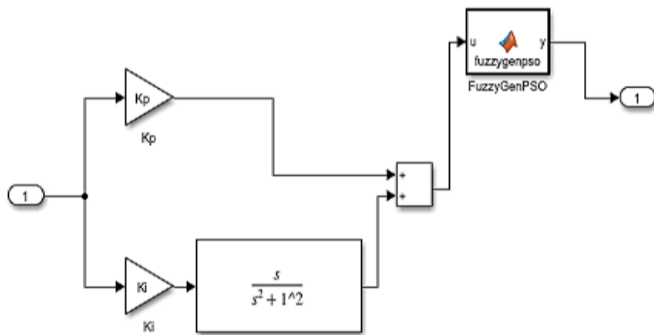


Fig. 5. Block diagram of the Fuzzy GPSOPR controller

The disadvantage of the Genetic Algorithm (GA) is that when the number of factors calculated for optimization it gets in to a complex state and difficulty in calculation increases, and thereby the calculation time also increases. PSO is used more than other algorithms as it is easy to implement. As a result, the algorithm is a popular method for solving optimization issues in the field of HRES. PSO is a strong contender for the convergent algorithm because of its ease of use, versatility, and minimal storage requirements, as well as its rapid convergence speed. The optimization of HRES' load is frequently an optimization problem with multiple conflicting objectives that must be resolved in order to arrive at a solution.

In this context, GA and PSO can help ensure consistent load by reducing steady state error and harmonics to reach the coordinated response exclusive of the risk of becoming stranded in local optimal solution, as classical optimization

approaches can. Finding near- optimal solutions is a common part of solving optimization problems. As a result, it is preferable to utilize an algorithm that can provide approximate solutions that are closer to the global optima. In this view, the heuristic character of GA and PSO, as well as the Fuzzy inference system method, may be summarized in the area of HRES load management as well as measurement due to their ability to reduce steady state error and harmonic as well as create constant load.

Fast convergence, imprecise input, and nonlinearity handling are advantages of FL. As shown in Figure 6, FL consists of three stages: fuzzification, rule basis lookup table, and defuzzification.

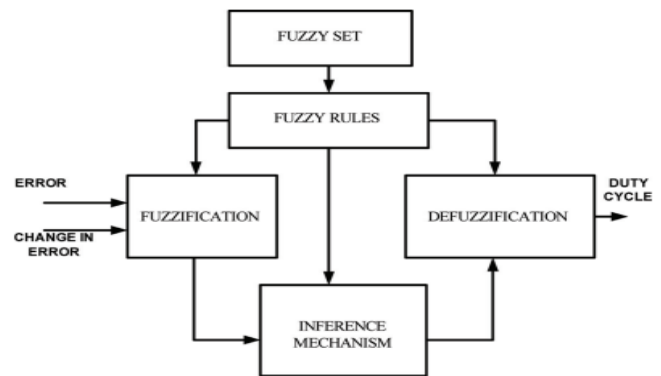


Fig. 6. Block diagram of the Fuzzy Logic

The rules are made on the system's previous history. An artificial closed-loop decision-making controller is known as an FLC. The error signal and the change in the error signal are given as the inputs for fuzzy controllers. Once the signals have been calculated and the linguistic variables have been retrieved, the output variable is determined using the rules mechanism. The precision and convergence speed of any FLC controller are determined by the membership function of input and output variables. In this research, the triangle membership function is utilized since it is easier to implement than the Gaussian and Trapezoidal membership functions.

The inputs of FL are preliminary values of parameters and as expressed in Eq. (22) and (23) respectively and output variable of the FL is the Change in DC voltage. These variables are represented in form of membership function as NL, NM, NS, ZO, PS, PM, PL. the fuzzification stage is employed with Sugeno's model and defuzzification utilizes the Weighted Average to calculate the output variable value.

$$k_p = k_{p0} + \Delta k_p \tag{22}$$

$$k_i = k_{i0} + \Delta k_i \tag{23}$$

The fuzzy mapping of input and output is carried based on Table 1. where  $(k_{p0}, k_{i0})$  are the input variables,  $(\Delta k_p, \Delta k_i)$  is the control variable and NL, NM, NS, ZO, PS, PM, PL are the fuzzy sets. Inference mechanism is basically defined by membership functions of FLC which determines the relevance of rules.

Table 1 Rule base of fuzzy controller.

e / Δe	NL	NM	NS	ZO	PS	PM	PL
--------	----	----	----	----	----	----	----



NL	PL	PL	PM	PS	NL	NL	NL
NM	PM	PM	PM	ZO	NM	NM	NM
NS	PM	PM	PS	ZO	NS	NS	NM
ZO	NS	NS	NS	ZO	PS	PS	PS
PS	NM	NM	NM	ZO	PS	PS	PM
PM	NM	NL	NM	ZO	PM	PM	PM
PL	NL	NL	NL	NS	PL	PM	PL

After completing FL, the output of FL is adjusted by GPSO. The flow chart of GPSO algorithm is shown in Fig. 7.

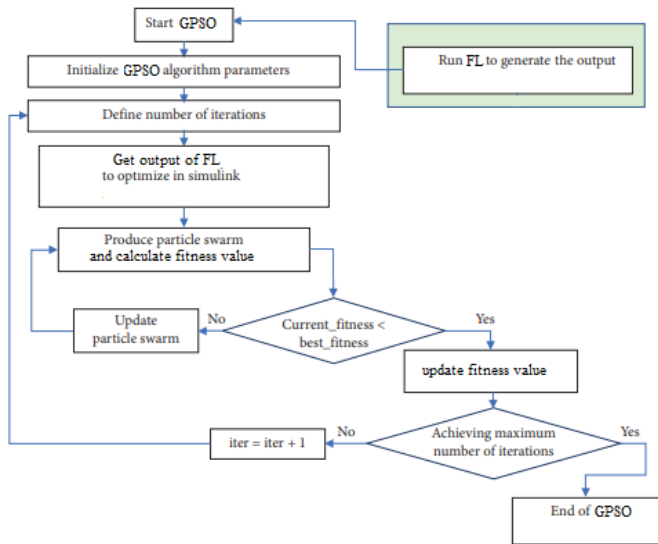


Fig. 7. Flow chart of GPSO algorithm

The pseudo-code for the GPSO algorithm is presented as follows:

1. Get the output voltage of Fuzzy logic and set these output voltage values as initial particles of GPSO.
2. Initially, assign all particles as Pbest and Gbest.
3. Calculate the fitness of each particle.
4. Evaluate if the current fitness is better than the current Pbest for each particle; if it is, update Pbest.
5. Calculate if any of the current pbests are better than the current Gbest. If any is, update Gbest with the best one.
6. Until the optimal voltage found, perform the following steps:
  - a. Upgrade the velocity of each particle and perform limit checks.
  - b. Upgrade the position of each particle according to the particle's velocity and perform limit checks.
7. Calculate the fitness of each particle.
8. If the limits have been reached, then stop. Else, loop back to step #4.

2.8. PWM Inverter

To convert dc to ac, a sinusoidal PWM converter is employed. A Fourier analysis can be used to examine the modulation phase voltage. Only the inverter's fundamental harmonic is examined here. The formula below can be used to compute the primary distortion of the voltage source inverter.

$$V_{ph}(t) = mV_{dc} \sin(\omega t) / 2 \tag{24}$$

Where m is the modulation index and Vph is the phase voltage's fundamental harmonic. If the inverter is efficient and the resonant frequencies in the output current are ignored, then DC and AC powers at the inverter sides are identical.

2.9. Energy Storage System BESS

A BESS is an energy storage system (ESS) which collects energy from multiple and then it is stored in rechargeable a battery which is then used when required. Multiple battery banks are incorporated to individual sources independently in the proposed model which is used to store the generated energy from solar and wind. Then the generated energy is fed to the load with the help of a hybrid battery management system. The battery bank may be in charge, discharge, or floating state that is based on the energy supplied to the battery by the sources as well as the power supplied by the battery to the load. The battery bank is connected to the load on the condition that the generated energy by the sources is less than the predefined value. When the total amount of power that is generated by PV and Wind becomes high, the energy is stored in a battery which is later connected to the load to meet the consumer's needs.

3. Results and Examination

3.1. Simulation Setup

Using Matlab Simulink 2019 a, a fuzzy GPSO based PR controller is simulated to evaluate the efficiency of the proposed methodology and also compared with the simulation results of fuzzy based PI, PR controllers in terms of steady state errors and harmonics.

Table 2 lists the simulation parameters utilized in these experiments.

Parameter	Value	Units
Wind turbine		
Number of blades	3	
Wind Speed	8 to 12	m/s
Pitch Angle	1 to 5	degree
Solar		
Temperature	15 to 35	Celsius degree

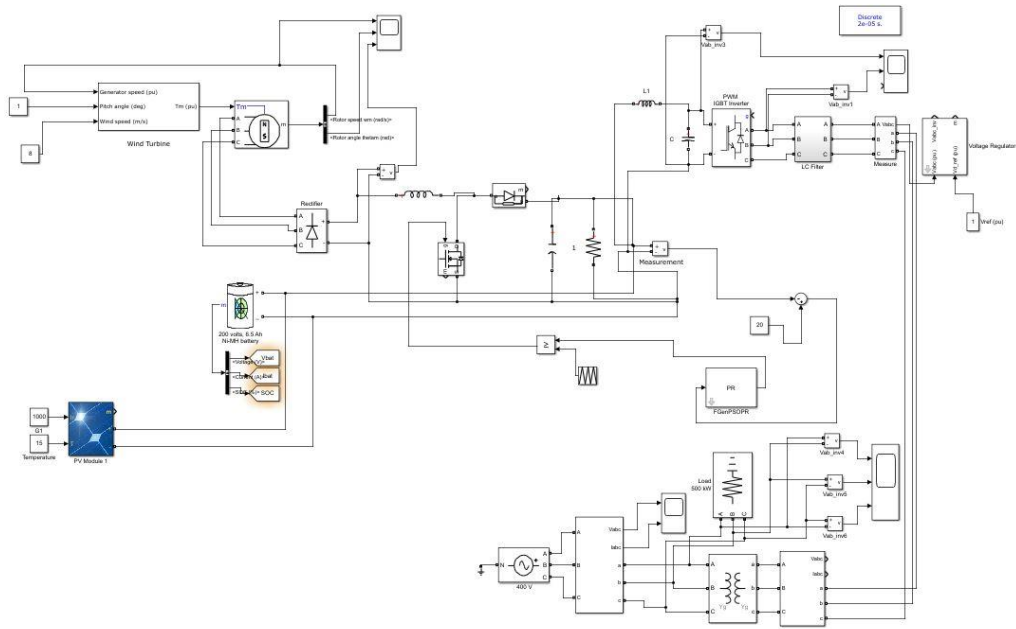


**Fig. 8.** Simulation diagram of Fuzzy based GPSO PR Controller

Fig. 8 depicts the simulation diagram of a Fuzzy based GPSO PR controller, whereas.

Fig. 9 depicts the simulation diagram of a Fuzzy based PI/PR controller.

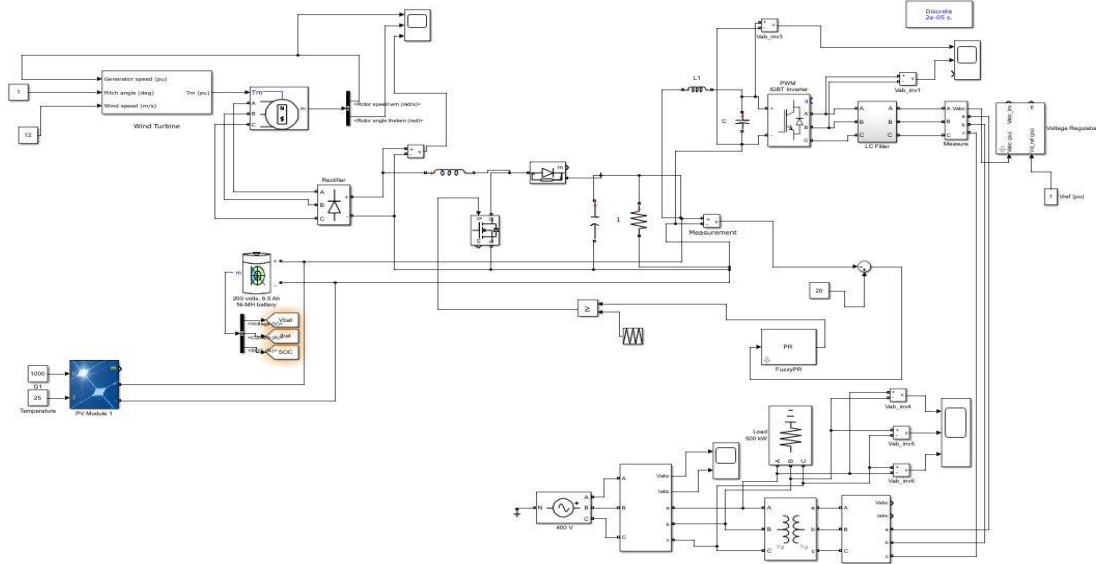


**Fig. 9.** Simulation diagram of Fuzzy based PI, PR Controller

### 3.2. Examination Parameters

A number of assessment parameters are available to test the efficacy of the Fuzzy based GPSO PR controller and Fuzzy based PI/PR Controller. The success of this work is evaluated using the steady state error and total harmonic distortion.

#### 3.2.1. Steady State Error

The difference between an energy-generating system's input and output in the limit as time approaches infinity is known as steady-state error (i.e., when the response has

reached steady state). Depending on the input, the steady-state error will vary (step, ramp, etc.)

#### 3.2.2. Total Harmonic Distortion

Total harmonic distortion is defined as the ratio of the sum of the powers of all harmonic components to the power of the fundamental frequency (THD).

### 3.3. Simulation Results

Fig. 10, 11, and 12 demonstrate the THD waveforms of load voltage as well as current handled through the fuzzy based PI controller.

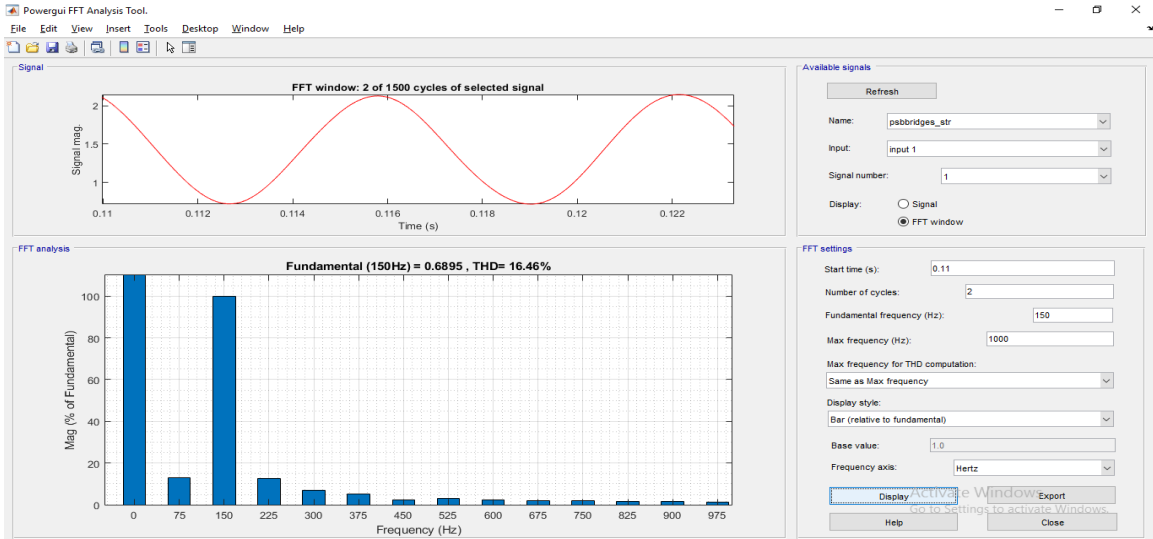


Fig. 10. THD waveform of Fuzzy PI Controller with wind speed 8 , Pitch angle 1, Temperature 15

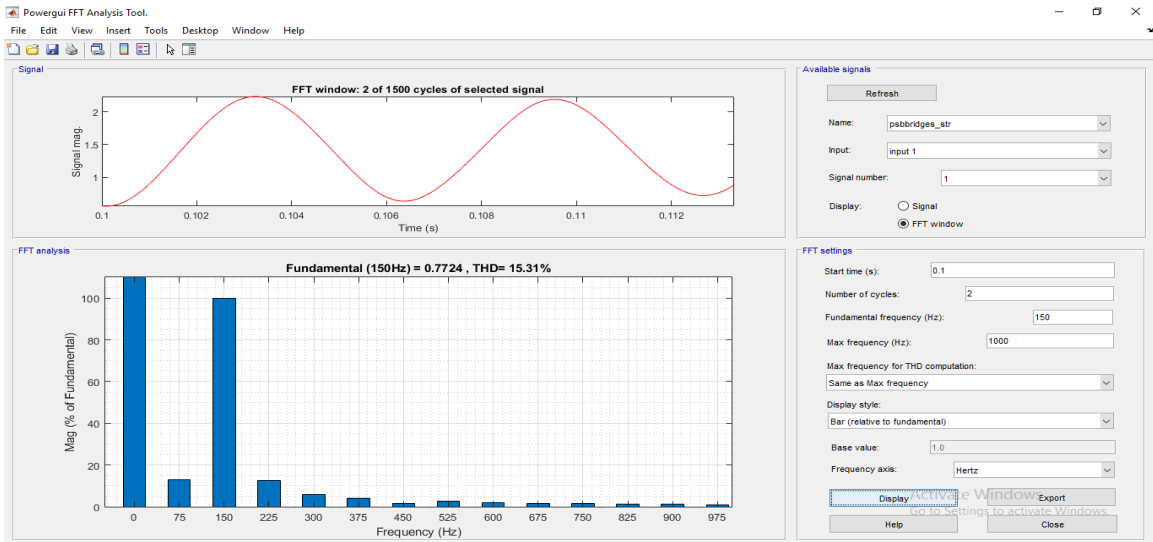


Fig. 11. THD waveform of Fuzzy PI Controller with wind speed 10, pitch angle 1, Temperature 20

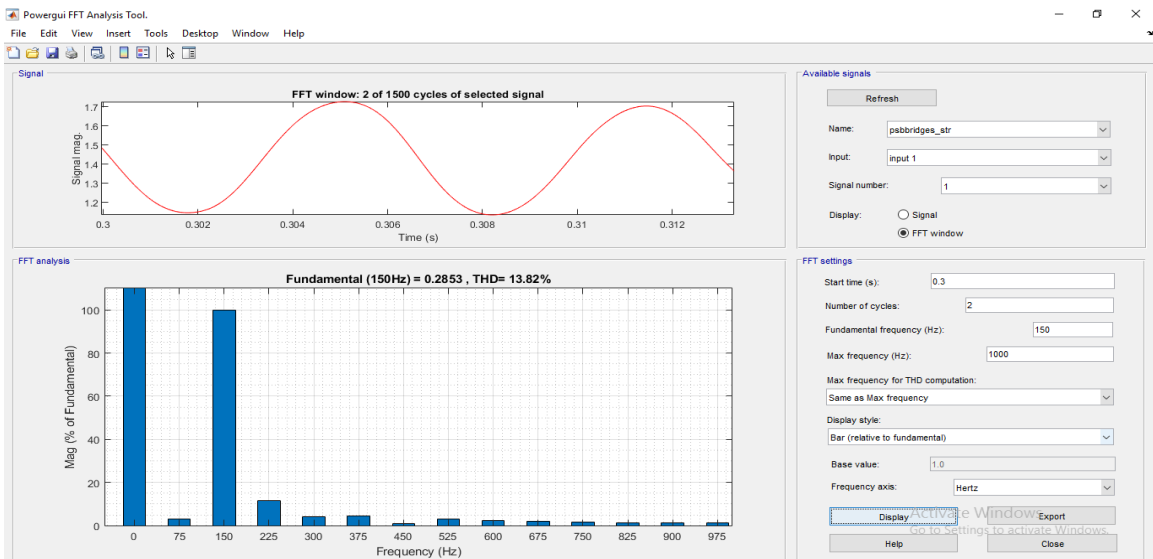
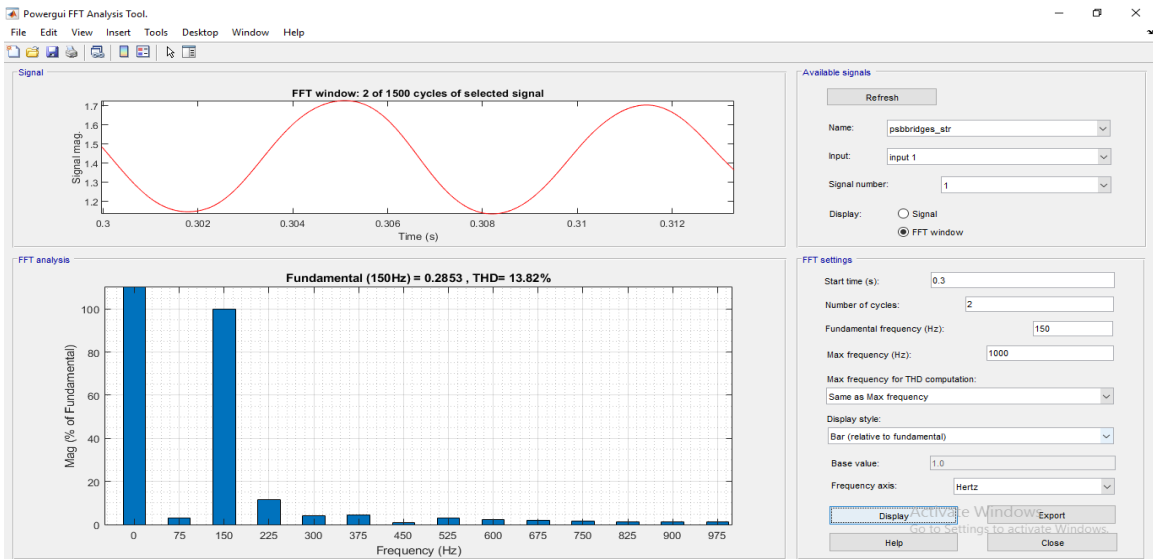


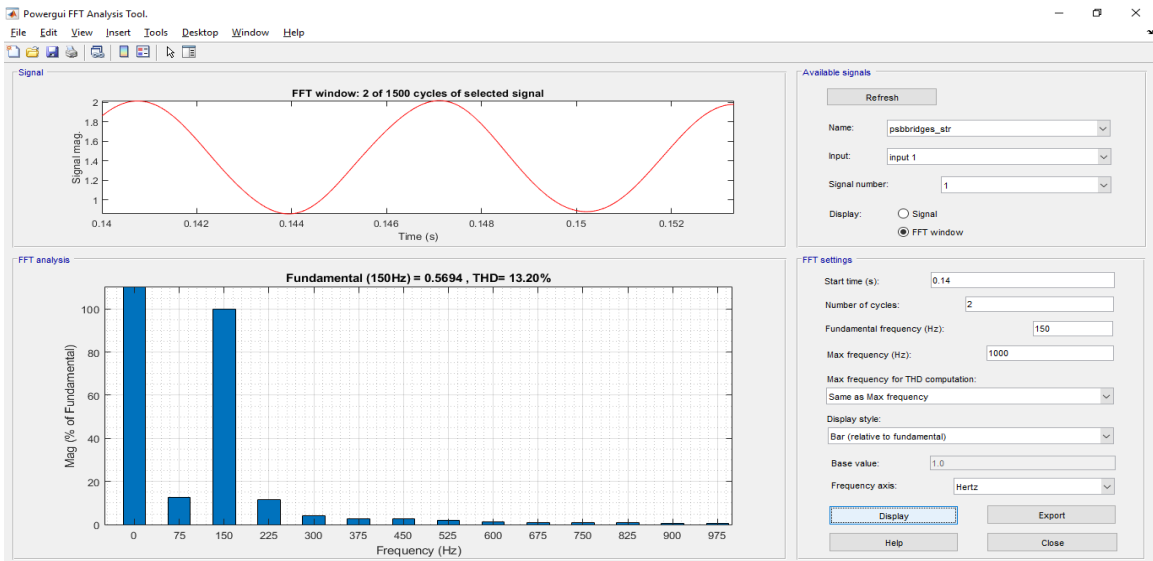
Fig. 12. THD waveform of Fuzzy PI Controller with wind speed 12, pitch angle 1, Temperature 25



Fig. 13, 14, and 15 demonstrate the THD waveforms of load voltage as well as current handled through the Fuzzy PR controller.



**Fig. 13.** THD waveform of Fuzzy PR Controller with wind speed 8, pitch angle 1, Temperature 15



**Fig. 14.** THD waveform of Fuzzy PR Controller with wind speed 10, pitch angle 1, Temperature 20

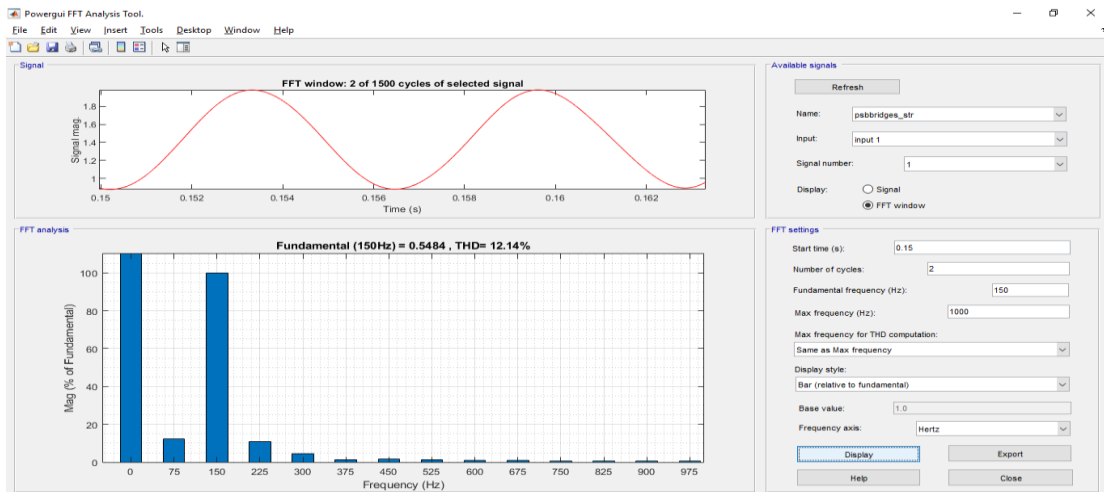


**Fig. 15.** THD waveform of Fuzzy PR controller with wind speed 12, pitch angle 1, Temperature 25

The THD waveforms of load voltage as well as current handled through Fuzzy GPSOPR controller are shown in Fig's 16, 17, and 18.

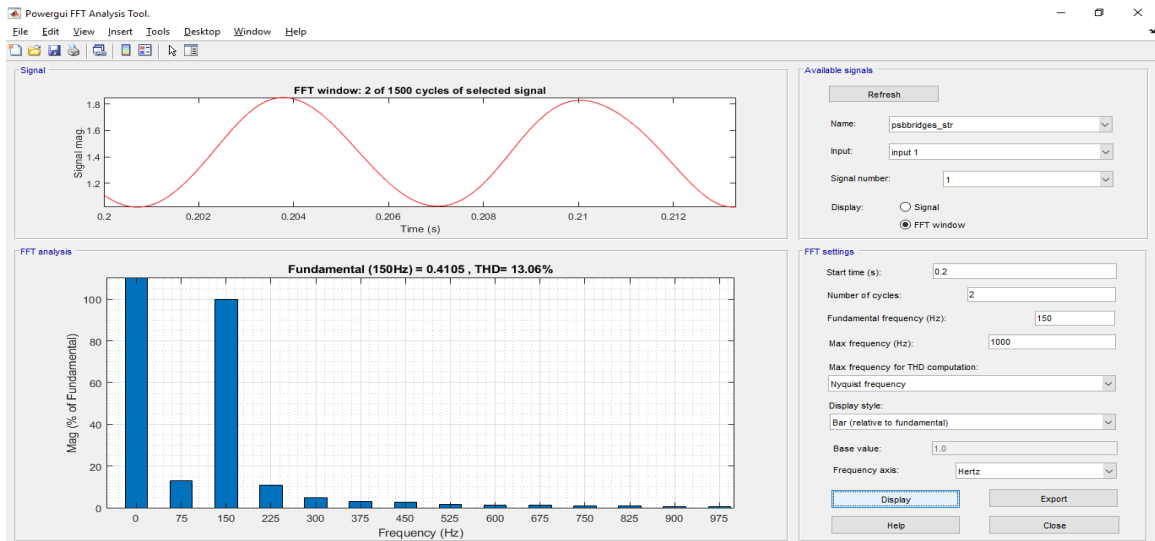


**Fig. 16.** THD waveform of FGPSO PR Controller with wind speed 8, pitch angle 1, Temperature 15

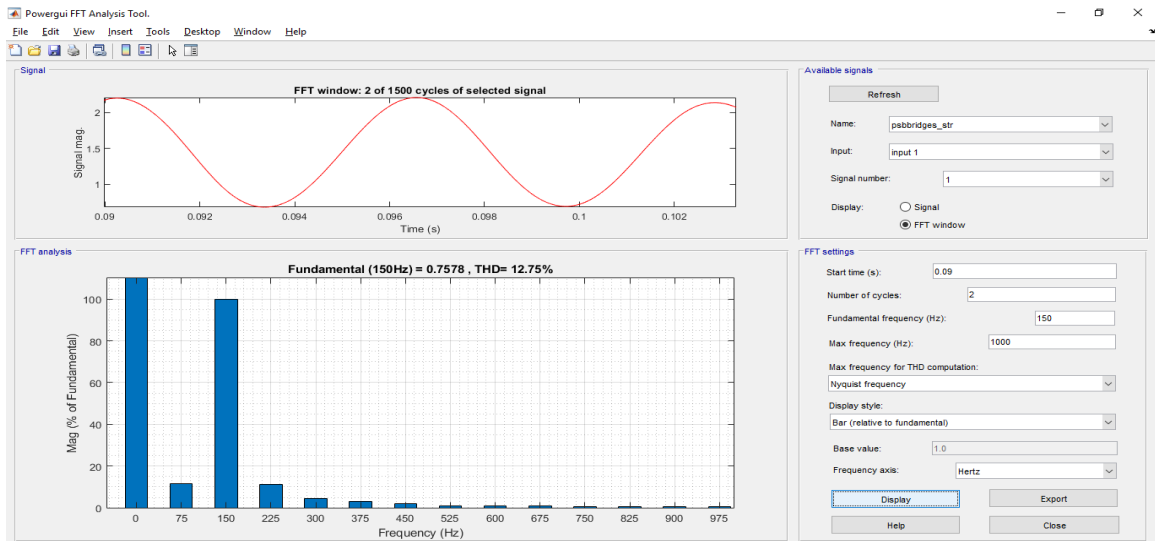


**Fig. 17.** THD waveform of FGPSO PR Controller with wind speed 10, pitch angle 1, Temperature 20

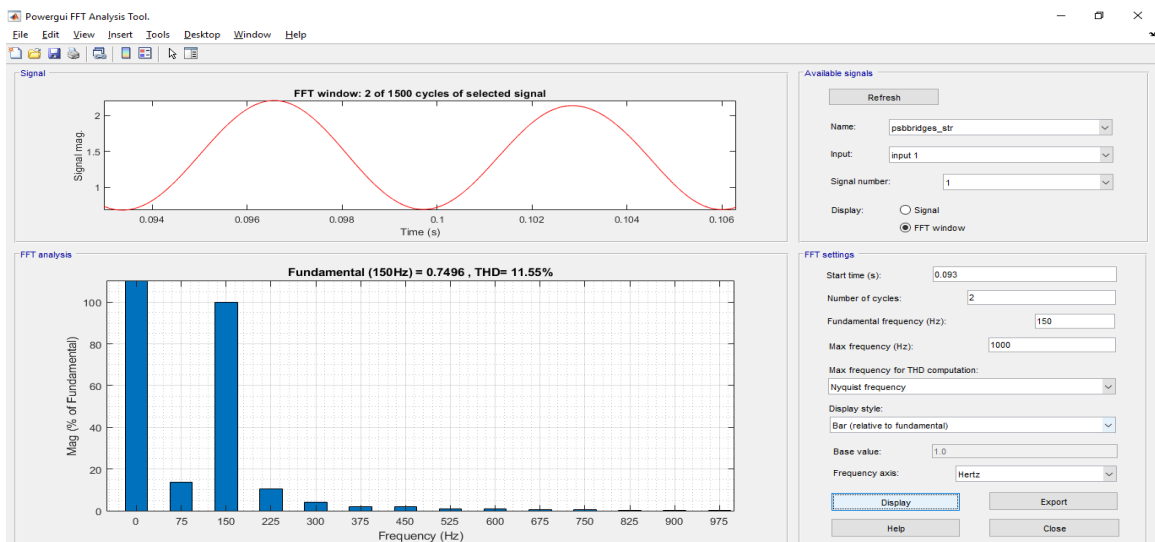


**Fig. 18.** THD waveform of FGPSO PR Controller with wind speed 12, pitch angle 1, Temperature 25

3.3.1. Trail No 1: Examination of Fuzzy GPSO-based PR Controller & Fuzzy-based PI, PR Controller Approaches Using Steady State Error

Using the operating indicators provided in Section 3.1, the effectiveness of the Fuzzy GPSO based PR controller is evaluated with the results of the Fuzzy based PI and PR controllers in terms of steady state errors. Table 3 summarizes the results of these indicators.

Table 3: Examination of Fuzzy GPSO based PR controller, Fuzzy based PI & PR controller using Steady State Error

	Wind Speed (WS) & PV Temperature (T)		
	WS=8 T=15	WS=10 T=20	WS=12 T=25
Fuzzy PI	0.0197	0.0259	0.0322
Fuzzy PR	0.0152	0.0214	0.0277
<b>Fuzzy GPSOPR</b>	<b>0.0147</b>	<b>0.0210</b>	<b>0.0273</b>

From Table 3 it is evident that, Fuzzy GPSO based PR controller has less steady state error than Fuzzy based PI, PR controller.

Fig. 19, 20 & 21 shows the Inverter voltage graphs of Fuzzy PR Controller at different wind speeds, pitch angle & solar temperatures.

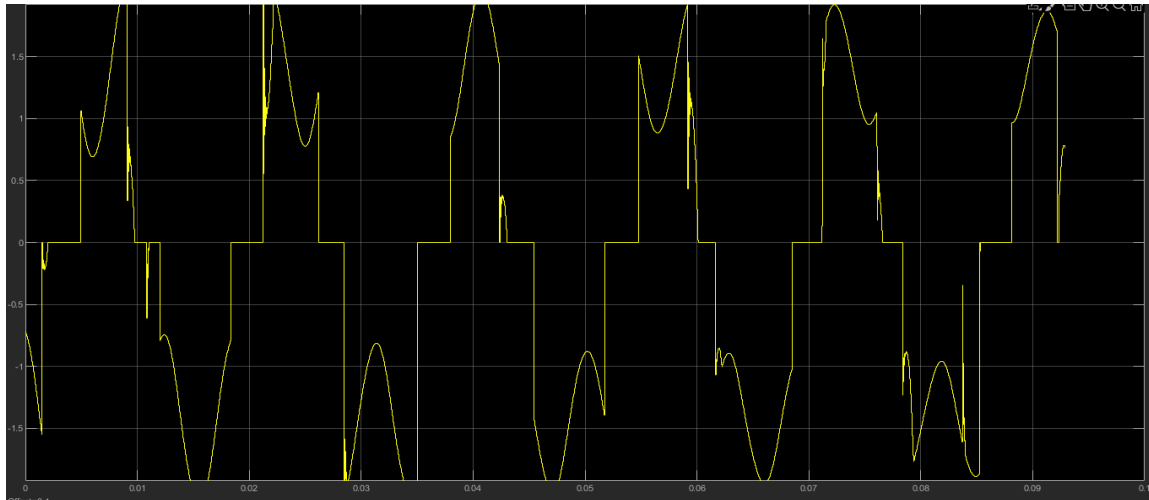


Fig. 19. Inverter Voltage at Wind Speed 8, Pitch angle 1 & Temperature 15

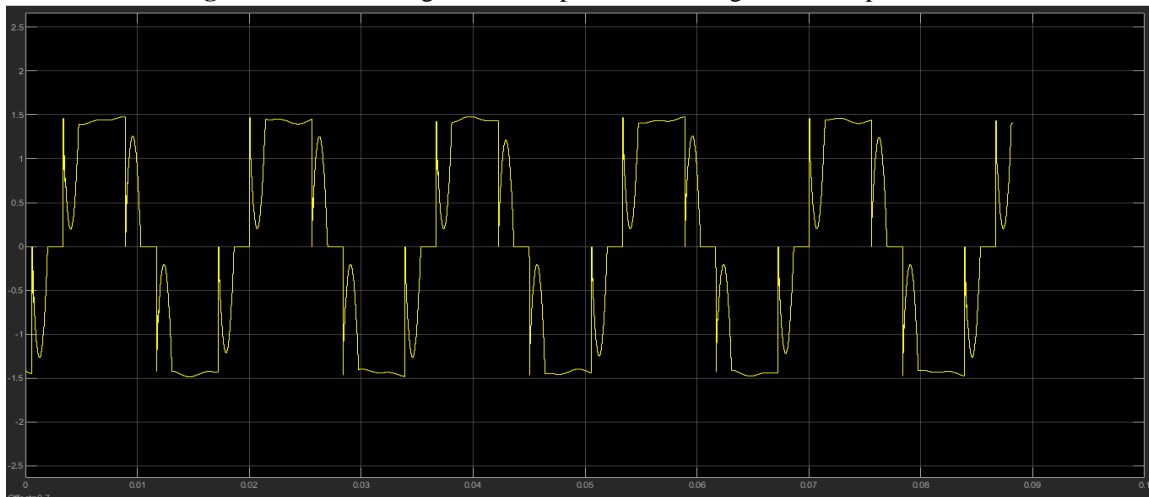


Fig. 20. Inverter Voltage at Wind Speed 10, Pitch angle 1 & Temperature 20

3.3.2. Trail No 2: Examination of Fuzzy GPSO-based PR Controller and Fuzzy-based PI, PR Controller Approaches Using Total Harmonic Distortion

Using the operating indicators listed in Section 3.1, the performance of the Fuzzy GPSO based PR controller is compared to that of the Fuzzy based PI, PR controller in terms of THD. Table 4 summarizes the results of these indicators.

Table 4: Examination of Fuzzy GPSO based PR controller and Fuzzy based PI, PR controller using total harmonic distortion

	Wind Speed (WS) & PV Temperature (T)		
	WS=8 T=15	WS=10 T=20	WS=12 T=25
Fuzzy PI	16.46	15.31	13.82
Fuzz PR	14.89	13.20	12.14
<b>Fuzzy GPSOPR</b>	<b>13.06</b>	<b>12.75</b>	<b>11.55</b>

From the table 4 it is evident that, Fuzzy GPSO based PR controller has lower THD than Fuzzy based PI, PR controller.

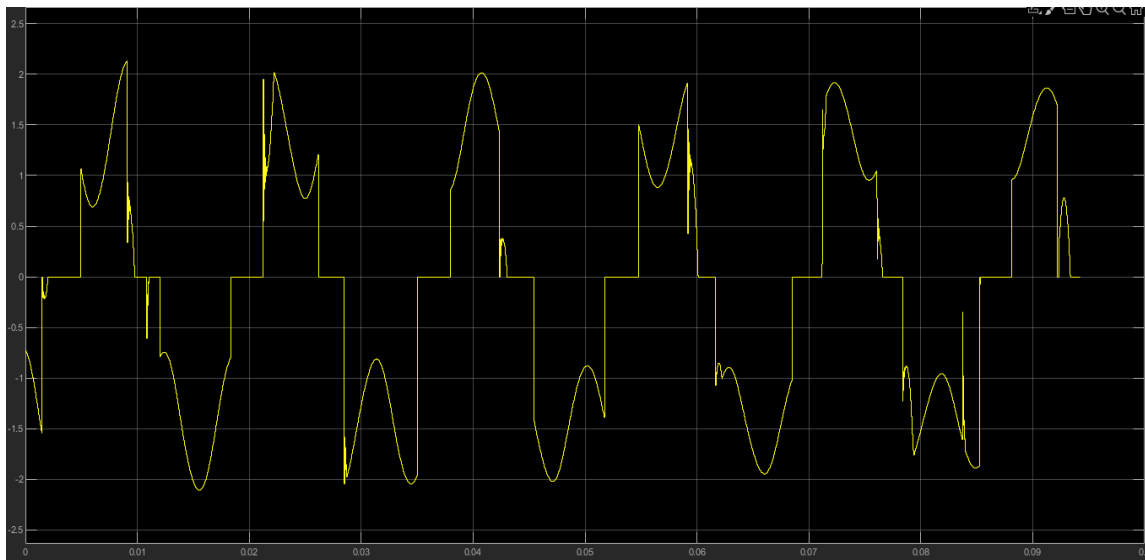


**Fig. 21.** Inverter Voltage at Wind Speed 10, Pitch angle 1 & Temperature 20

Fig. 22, 23 & 24 shows the Inverter voltage graphs of Fuzzy GPSO PR Controller at different wind speeds, pitch angle & solar temperatures.

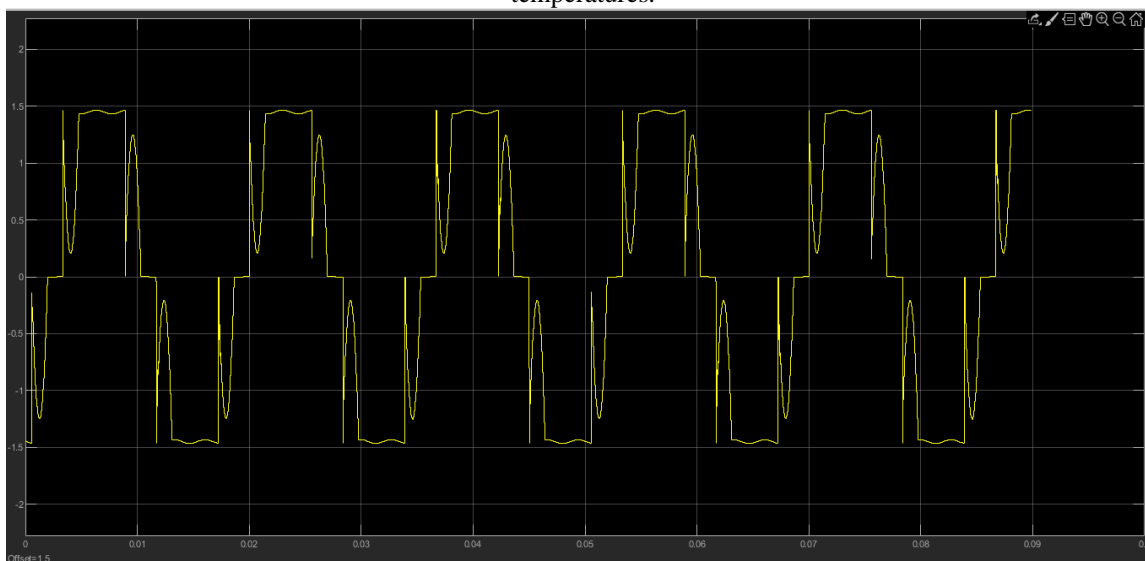


**Fig. 22.** Inverter Voltage at Wind Speed 8, Pitch angle 1 & Temperature 15

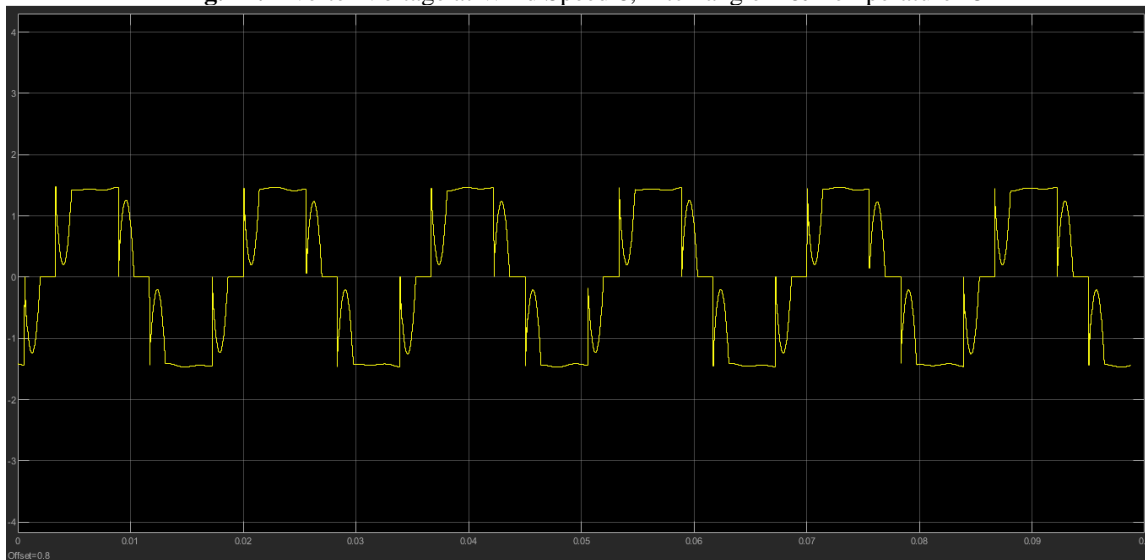


**Fig. 23.** Inverter Voltage at Wind Speed 10, Pitch angle 1 & Temperature 20

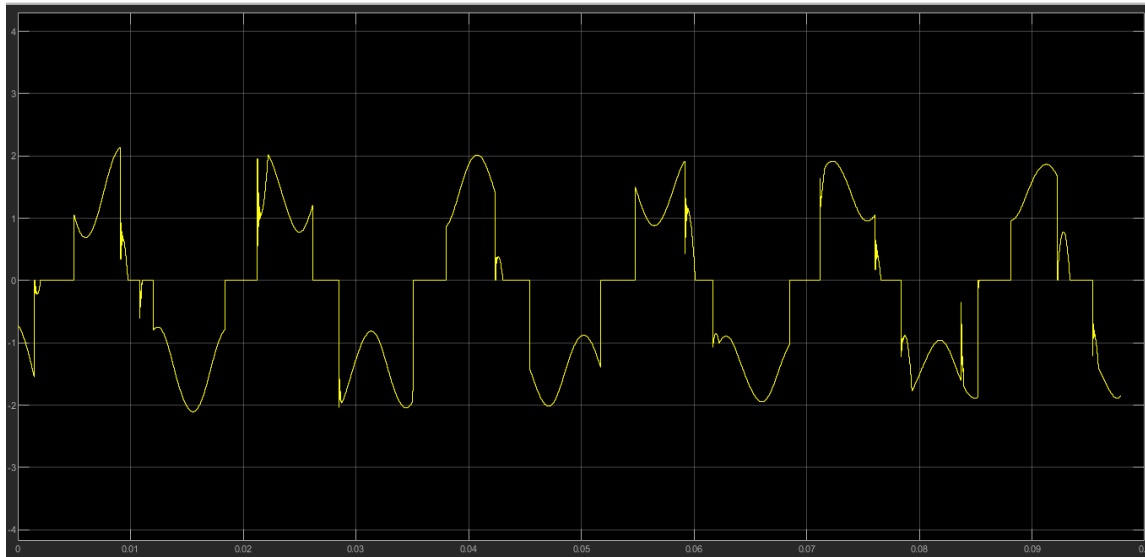


**Fig. 24.** Inverter Voltage at Wind Speed 10, Pitch angle 1 & Temperature 20

#### 4. Conclusion

For enhanced voltage regulation assistance in freestanding hybrid power systems, this paper suggested a Fuzzy GPSO based Proportional Resonant controller. In the synchronized control system, a PR controller was used instead of a traditional PI controller. A fuzzy GPSO controller was used to optimize the gain values of the PR controller. The suggested Fuzzy GPSOPR coordinated controller was compared with Fuzzy PI, PR controller by using evaluation metrics like steady state error and harmonics. In terms of delivering the constant output voltage, the recommended Fuzzy GPSOPR performs better than the Fuzzy PI, PR controller. Furthermore, the Fuzzy GPSO PR controller has a relatively low THD and steady state error when opposed to the Fuzzy PI, PR controller. The system's performance was validated using the MATLAB/SIMULINK tool.

#### References

- [1] X. yan Jiang, C. He, and K. Jermsittiparsert, "Online optimal stationary reference frame controller for inverter interfaced distributed generation in a microgrid system," *Energy Reports*, vol. 6, pp. 134–145, Nov. 2020, doi: 10.1016/J.EGYR.2019.12.016.
- [2] D. Sattianadan, S. Gorai, G. R. Prudhvi Kumar, S. Vidyasagar, and V. Shanmugasundaram, "Potency of PR controller for multiple harmonic compensation for a single-phase grid connected system," *Int. J. Power Electron. Drive Syst.*, vol. 11, no. 3, pp. 1491–1498, Sep. 2020, doi: 10.11591/IJPEDES.V11.I3.PP1491-1498.
- [3] Y. W. Kean, A. Ramasamy, S. Sukumar, and M. Marsadek, "Adaptive Controllers for Enhancement of Stand-Alone Hybrid System Performance," *Int. J. Power Electron. Drive Syst.*, vol. 9, no. 3, pp. 979–986, Sep. 2018, doi: 10.11591/IJPEDES.V9.I3.PP979-986.
- [4] M. Salimi, F. Radmand, and M. H. Firouz, "Dynamic Modeling and Closed-loop Control of Hybrid Grid-connected Renewable Energy System with Multi-input Multi-output Controller," *J. Mod. Power Syst. Clean Energy*, vol. 9, no. 1, pp. 94–103, Jan. 2021, doi: 10.35833/MPCE.2018.000353.
- [5] F. S. Tidjani, A. Hamadi, A. Chandra, P. Pillay, and A. Ndtoungou, "Optimization of Standalone Microgrid Considering Active Damping Technique and Smart Power Management Using Fuzzy Logic Supervisor," *IEEE Trans. Smart Grid*, vol. 8, no. 1, pp. 475–484, Jan. 2017, doi: 10.1109/TSG.2016.2610971.
- [6] M. Faisal, M. A. Hannan, P. J. Ker, M. S. A. Rahman, R. A. Begum, and T. M. I. Mahlia, "Particle swarm optimised fuzzy controller for charging–discharging and scheduling of battery energy storage system in MG applications," *Energy Reports*, vol. 6, pp. 215–228, Dec. 2020, doi: 10.1016/J.EGYR.2020.12.007.
- [7] L. El Boujdaini, A. Mezrhab, M. A. Moussaoui, F. Jurado, and D. Vera, "Sizing of a stand-alone PV–wind–battery–diesel hybrid energy system and optimal combination using a particle swarm optimization algorithm," *Electr. Eng.*, vol. 104, no. 5, pp. 3339–3359, Oct. 2022, doi: 10.1007/S00202-022-01529-0/FIGURES/17.
- [8] A. Razmjoo, R. Shirmohammadi, A. Davarpanah, F. Pourfayaz, and A. Aslani, "Stand-alone hybrid energy systems for remote area power generation," *Energy Reports*, vol. 5, pp. 231–241, Nov. 2019, doi: 10.1016/J.EGYR.2019.01.010.
- [9] G. Pathak, B. Singh, and B. K. Panigrahi, "Wind-Hydro microgrid and its control for rural energy system," *India Int. Conf. Power Electron. IICPE*, vol. 2016–November, Jun. 2016, doi: 10.1109/IICPE.2016.8079374.

- [10] S. Vadi, F. B. Gurbuz, S. Sagioglu, and R. Bayindir, "Optimization of PI based buck-boost converter by particle swarm optimization algorithm," 9th Int. Conf. Smart Grid, icSmartGrid 2021, pp. 295–301, Jun. 2021, doi: 10.1109/ICSMARTGRID52357.2021.9551229.
- [11] T. Dharma Raj and K. Chandrasekaran, "Dynamic performance improvement of buck-cuk converter in renewable energy resources using EHO optimised PR controller," IET Power Electron., vol. 13, no. 14, pp. 3009–3017, Nov. 2020, doi: 10.1049/IET-PEL.2020.0118.
- [12] N. Guler, "Proportional Resonant and Proportional Integral Based Control Strategy for Single Phase Split Source Inverters," 9th Int. Conf. Renew. Energy Res. Appl. ICRERA 2020, pp. 510–514, Sep. 2020, doi: 10.1109/ICRERA49962.2020.9242690.
- [13] S. Sinha and S. S. Chandel, "Review of recent trends in optimization techniques for solar photovoltaic-wind based hybrid energy systems," Renew. Sustain. Energy Rev., vol. 50, pp. 755–769, Oct. 2015, doi: 10.1016/J.RSER.2015.05.040.
- [14] S. Singh, M. Singh, and S. C. Kaushik, "Feasibility study of an islanded microgrid in rural area consisting of PV, wind, biomass and battery energy storage system," Energy Convers. Manag., vol. 128, pp. 178–190, Nov. 2016, doi: 10.1016/J.ENCONMAN.2016.09.046.
- [15] A. M. Eltamaly and M. A. Mohamed, "Optimal Sizing and Designing of Hybrid Renewable Energy Systems in Smart Grid Applications," Adv. Renew. Energies Power Technol., vol. 2, pp. 231–313, Jan. 2018, doi: 10.1016/B978-0-12-813185-5.00011-5.
- [16] [16] A. Colak and K. Ahmed, "A Brief Review on Capacity Sizing, Control and Energy Management in Hybrid Renewable Energy Systems," 10th IEEE Int. Conf. Renew. Energy Res. Appl. ICRERA 2021, pp. 453–458, 2021, doi: 10.1109/ICRERA52334.2021.9598654.
- [17] A. S. Aziz, M. F. N. Tajuddin, M. R. Adzman, M. A. M. Ramli, and S. Mekhilef, "Energy Management and Optimization of a PV/Diesel/Battery Hybrid Energy System Using a Combined Dispatch Strategy," Sustain. 2019, Vol. 11, Page 683, vol. 11, no. 3, p. 683, Jan. 2019, doi: 10.3390/SU11030683.
- [18] K. H. Chua, Y. S. Lim, and S. Morris, "A novel fuzzy control algorithm for reducing the peak demands using energy storage system," Energy, vol. 122, pp. 265–273, Mar. 2017, doi: 10.1016/J.ENERGY.2017.01.063.
- [19] S. Hadji, F. Krim, and J. P. Gaubert, "Development of an algorithm of maximum power point tracking for photovoltaic systems using genetic algorithms," 7th Int. Work. Syst. Signal Process. their Appl. WoSSPA 2011, pp. 43–46, 2011, doi: 10.1109/WOSSPA.2011.5931408.
- [20] R. Alkassem, M. Al Ahmadi, and A. Draou, "Modeling and simulation analysis of a hybrid PV-wind renewable energy sources for a micro-grid application," 9th Int. Conf. Smart Grid, icSmartGrid 2021, pp. 103–106, Jun. 2021, doi: 10.1109/ICSMARTGRID52357.2021.9551215.
- [21] V. O. Okinda and N. A. Odero, "A REVIEW OF TECHNIQUES IN OPTIMAL SIZING OF HYBRID RENEWABLE ENERGY SYSTEMS," IJRET Int. J. Res. Eng. Technol., pp. 2321–7308, Accessed: Nov. 23, 2022. [Online]. Available: <http://www.ijret.org>
- [22] N. H. Samrat, N. Bin Ahmad, I. A. Choudhury, and Z. Bin Taha, "Modeling, control, and simulation of battery storage photovoltaic-wave energy hybrid renewable power generation systems for island electrification in malaysia," Sci. World J., vol. 2014, 2014, doi: 10.1155/2014/436376.
- [23] B. Bhandari, S. R. Poudel, K. T. Lee, and S. H. Ahn, "Mathematical modeling of hybrid renewable energy system: A review on small hydro-solar-wind power generation," Int. J. Precis. Eng. Manuf. Technol. 2014 12, vol. 1, no. 2, pp. 157–173, Apr. 2014, doi: 10.1007/S40684-014-0021-4.
- [24] J. Ahmed and Z. Salam, "An improved perturb and observe (P&O) maximum power point tracking (MPPT) algorithm for higher efficiency," Appl. Energy, vol. 150, pp. 97–108, Jul. 2015, doi: 10.1016/J.APENERGY.2015.04.006.
- [25] J. Hui, A. Bakhshai, and P. K. Jain, "A hybrid wind-solar energy system: A new rectifier stage topology," Conf. Proc. - IEEE Appl. Power Electron. Conf. Expo. - APEC, pp. 155–161, 2010, doi: 10.1109/APEC.2010.5433678.
- [26] M. C. Sahbi Abderrahim, Moez Allouche, "A New Robust Control Strategy for a Wind Energy Conversion System Based on a T-S Fuzzy Model," Int. J. Smart grid, vol. Vol.4, No., no. June, 2020 A, pp. 88–99, 2020, doi: 10.20508/IJSMARTGRID.V4I2.103.G87.